Electronic Supplementary Information (ESI)

Three-dimensional hierarchical nitrogen-doped arch and hollow nanocarbons: Morphological influences in the supercapacitor applications

Prakash Ramakrishnan[a], Soo-Gil Park[b] and Sangaraju Shanmugam*[a]

[a] Department of Energy Systems Engineering,

Daegu Gyeongbuk Institute of Science & Technology (DGIST), Daegu, 711-873,

Republic of Korea. * E-mail: sangarajus@dgist.ac.kr, Fax: 82 53 785 6409.

[b] Department of Industrial Engineering Chemistry,

Chungbuk National University, Cheongju 361-763,

Republic of Korea.

Formulas applied in three electrode system:

The specific capacitance (C_{sp}) values obtained from CV are calculated using the equation (1)

$$C_{sp} = Q / m.v \ (F\ g^{-1}) \quad [1] \qquad -(1)$$

Where Q, m and v is the average current of anodic and cathodic current in mA, active material (mg), applied scan rate (mV s^{-1}), respectively**.**

The C_{sp} values for galvanostatic charge-discharge are calculated using the equation (2)

$$C_{sp} = I.\ \Delta t / m.V \ (F\ g^{-1})\ ^{1} \qquad -(2)$$

Where I, Δt, m and V represents the applied current density, discharge time, active mass and working potential window.

Formulas applied in two electrode system:

The C_{sp} values obtained from CV are calculated using the equation (3)

$$C_{sp} = 4\ Q / m.v \ [1] \qquad -(3)$$

Where, m is the total mass of the active material in both electrodes (mg), factor 4 is used to compensate the mass of a single electrode and capacitance of both electrodes.

The C_{sp} values for galvanostatic charge-discharge are calculated using the equation (4)

$$C_{sp} = 4\ I.\ \Delta t / m.V\ ^{1}. \qquad -(4)$$

The energy densities (E) and the power densities of all the materials were calculated using equation (5) and (6).

$$E = (C.V^2) / 8 \qquad ^{2} \quad -(5)$$

$$P = E/\Delta t \qquad ^{2} \quad -(6)$$

Where, C is the capacitance obtained from galvanostatic and discharge measurement, V is the working potential window and Δt is the discharge time.

Characterization

The field emission scanning electron microscope, S4800 FE-SEM, and field emission transmission electron microscope, HF 3600 FE-TEM were used for morphological analysis. The Raman spectroscopy with source wavelength of 514 nm and high resolution X-ray diffraction, HR-XRD were used to understand the graphitic phase of carbon nature. The elemental analyzer, EA Vario MICRI cube used for quantitative analysis of heteroatom functionalities. The X-ray photo-electron spectroscope, XPS Thermo scientific ESCALAB 250Xi, performed to unveil the chemical nature of heteroatom species. The Bruner–Emmett–Teller, BET Micromeritics ASAP 2020, were used to understand the surface area and micropore texture information: pore size distribution calculated from non-local density functional theory, NLDFT and micro texture information derived from t-plot method using Harkins and Jura formula. All the samples were degassed at 180 ^{o}C overnight in prior to analysis.

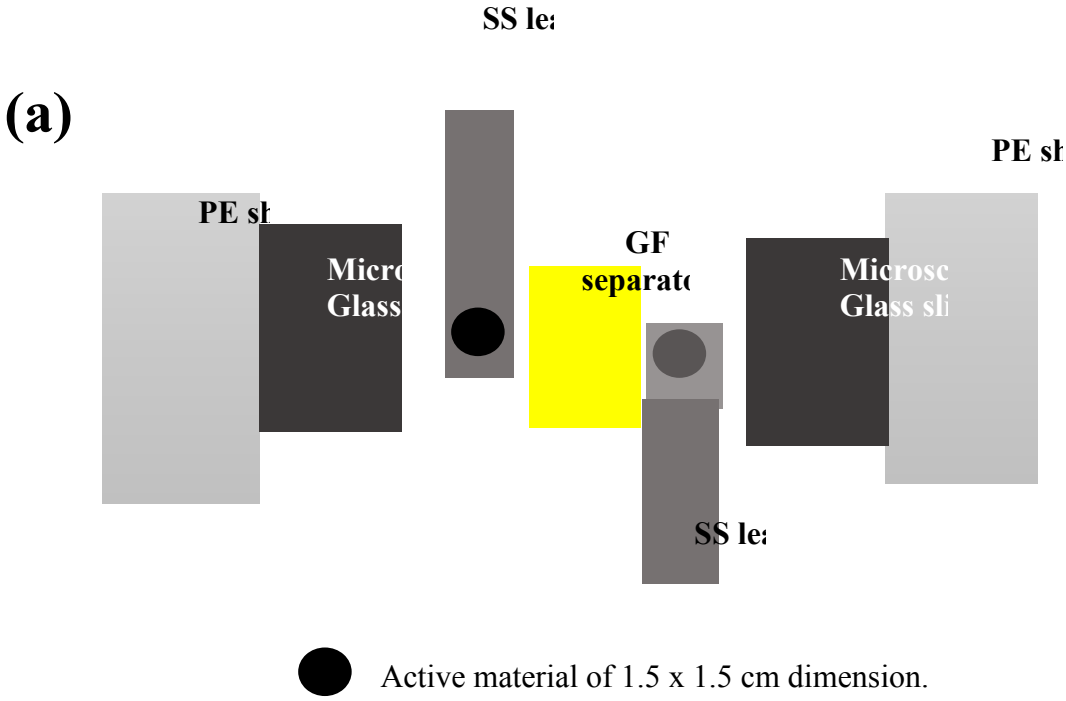

Fig. S1 (a) Symmetric two electrode configuration of the home made cell, (b) Photograph image of designed symmetric two electrode cell configuration system.

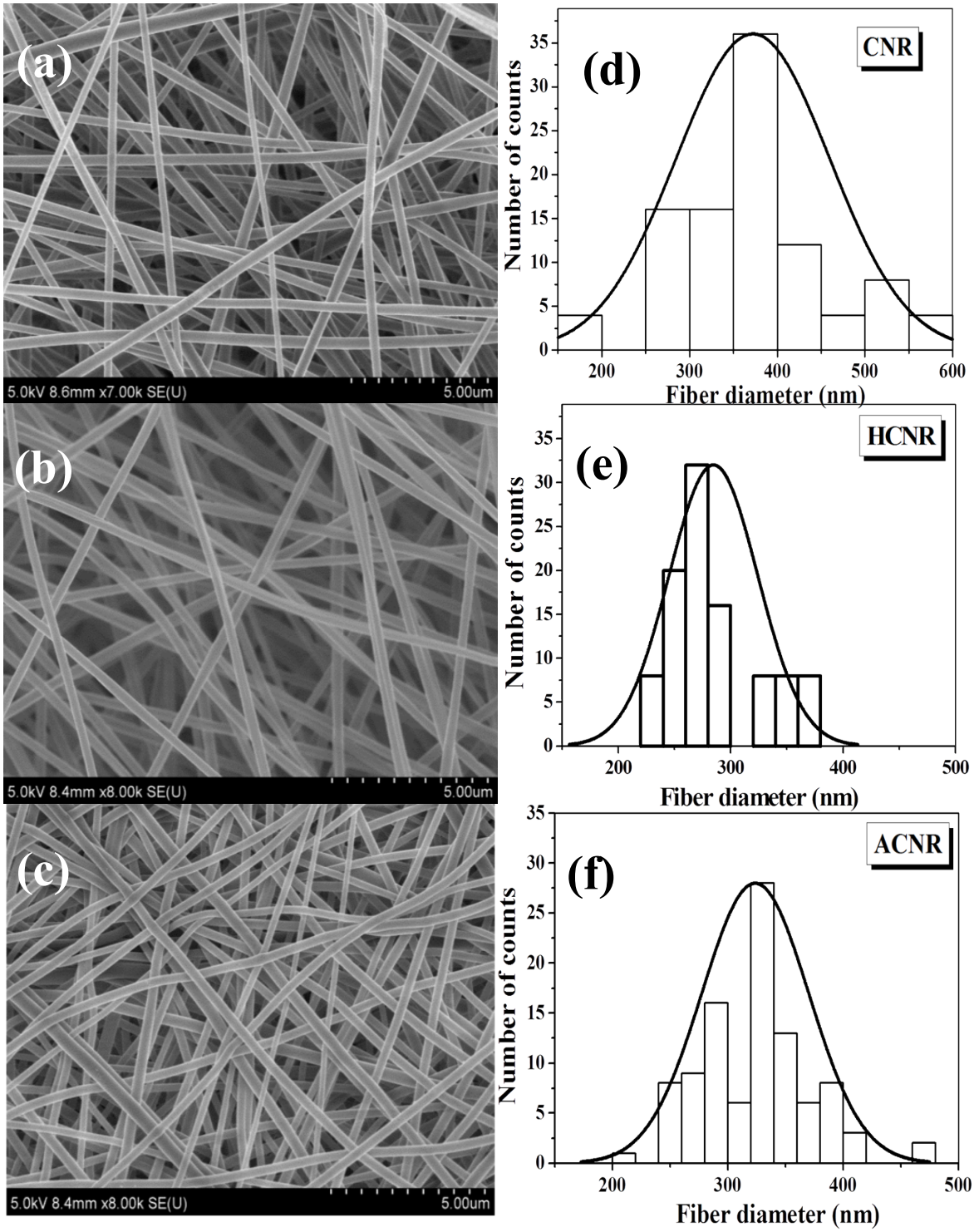

Fig. S2 FE-SEM images (a, b, c) of as prepared electrospun membrane and nanofiber diameter histogram (d, e, f) of CNR, HCNR and ACNR samples, respectively.

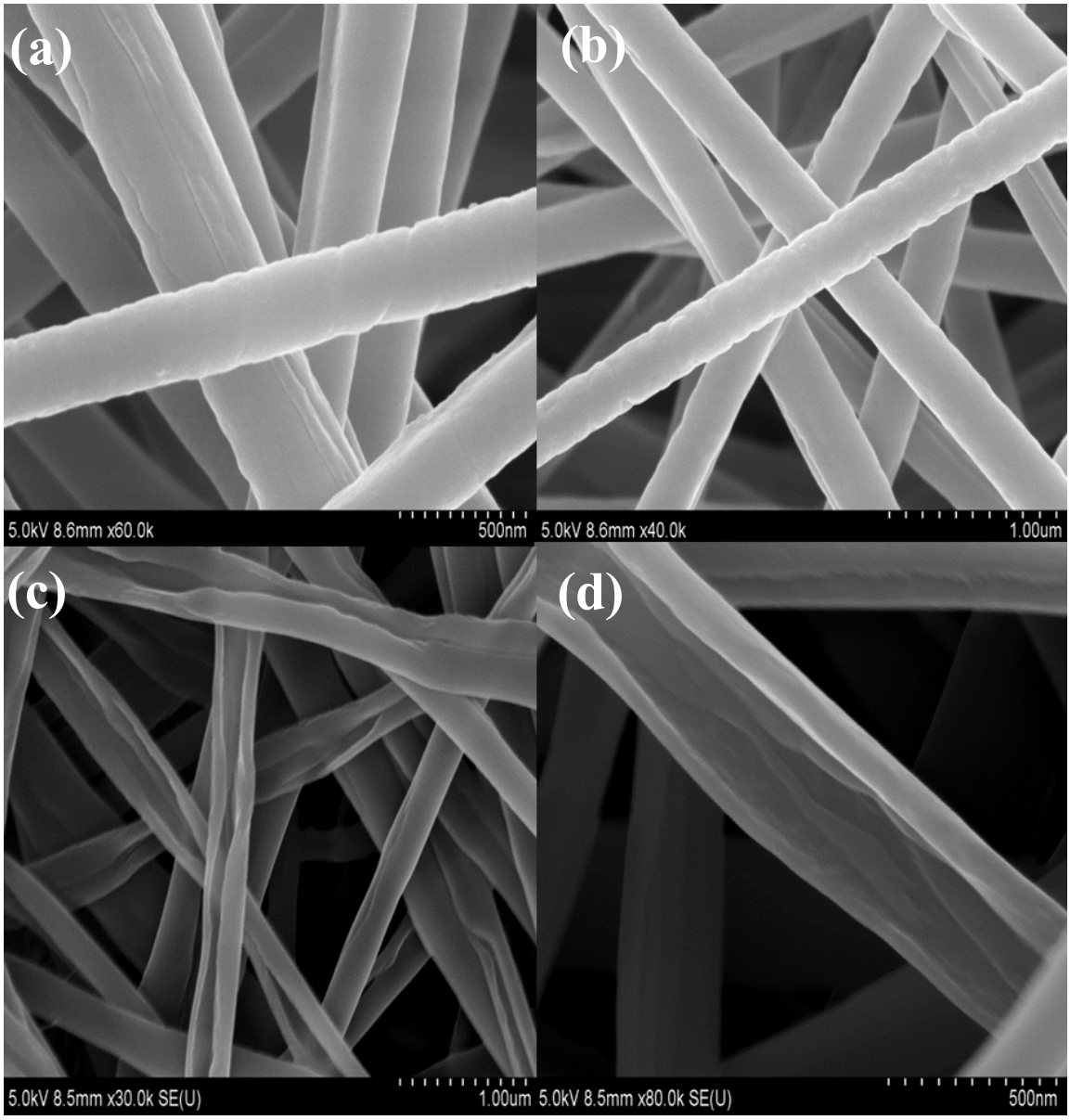

Fig. S3 FE-SEM images of water leached membranes of HCNR (a, b) and ACNR (c, d) samples, respectively.

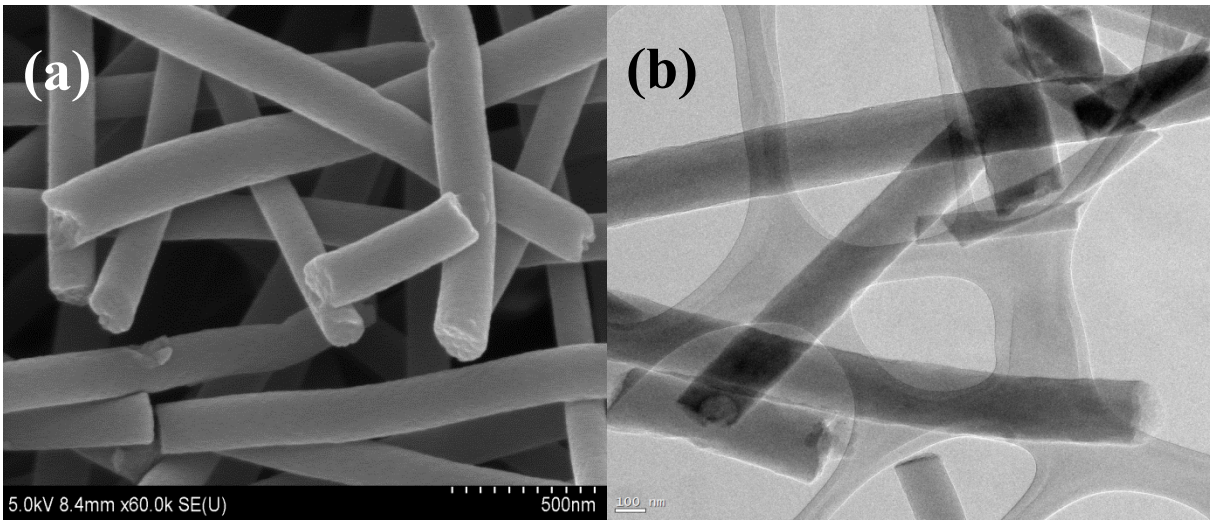

Fig. S4 (a)FE-SEM and (b) FE-TEM images of CNR sample.

Table S1. XPS deconvoluted values of C_{1s}, N_{1s} and O_{1s} for all samples.										
Samples	**C 1s**				**N 1s**		**O 1s**			
	C_1 (eV)	**C_2 (eV)**	**C_3 (eV)**	**C_4 (eV)**	**N_1 (eV)**	**N_2 (eV)**	**O_1 (eV)**	**O_2 (eV)**	**O_3 (eV)**	**O_4 (eV)**
CNR	284.4	285.0	285.4	286.6	398.4	401.0	530.6	531.5	532.4	533.6
HCNR	284.4	285.0	285.7	286.7	398.5	401.1	530.6	531.3	532.2	533.4
ACNR	284.5	285.1	285.6	286.5	398.4	401.1	530.6	531.3	532.4	533.4

Table S2. XPS deconvoluted area of C1 s spectra of all samples.						
Sample	**Area-C_1**	**Area-C_2**	**Area-C_3**	**Area-C_4**	**Total area**	**sp^2%**
CNR	10660.9	36806.0	29842.2	9735.2	87044.3	12%
HCNR	8366.4	35399.0	20793.8	14866.4	79425.6	11%
ACNR	15204.1	25459.9	17788.8	18027.8	76480.6	20%

Table S3. XPS deconvoluted area of N1 s spectra of all samples					
Sample	**Area-N_1**	**Area-N_2**	**Total area**	**N_1 (Pyridinic) %**	**N_2 (Graphitic/ Quaternary) %**
CNR	16842.0	11450.8	28292.8	39%	61%
HCNR	13459.3	8709.3	22168.6	40%	60%
ACNR	13683.3	6993.0	25685.3	46%	54%

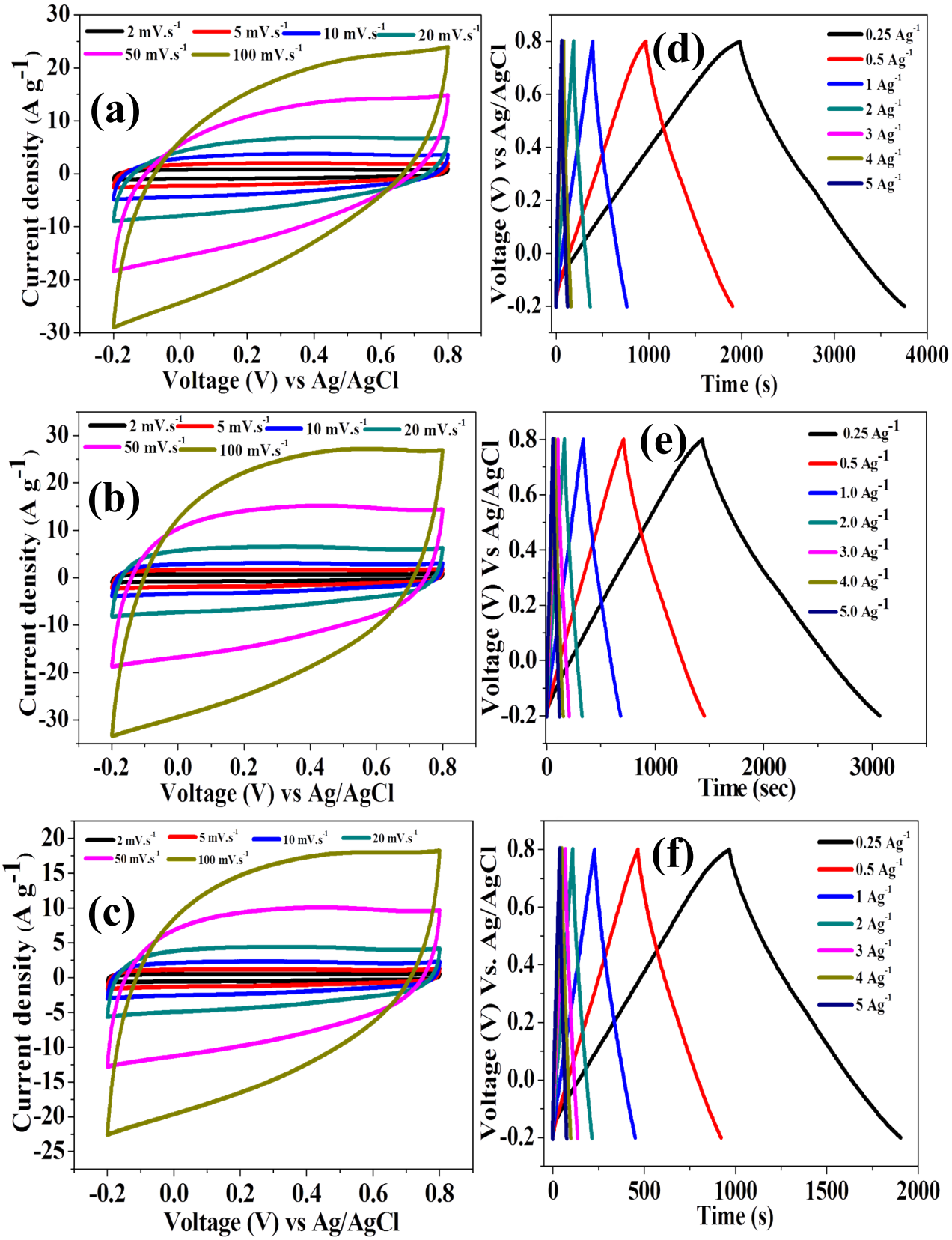

Fig. S5 Three electrode cell electrochemical anlaysis: (a) – (c) are CVs of ACNR, HCNR and CNR, respectively and (d) – (f) are galvanostatic charge-discharge profiles of ACNR, HCNR and CNR, respectively.

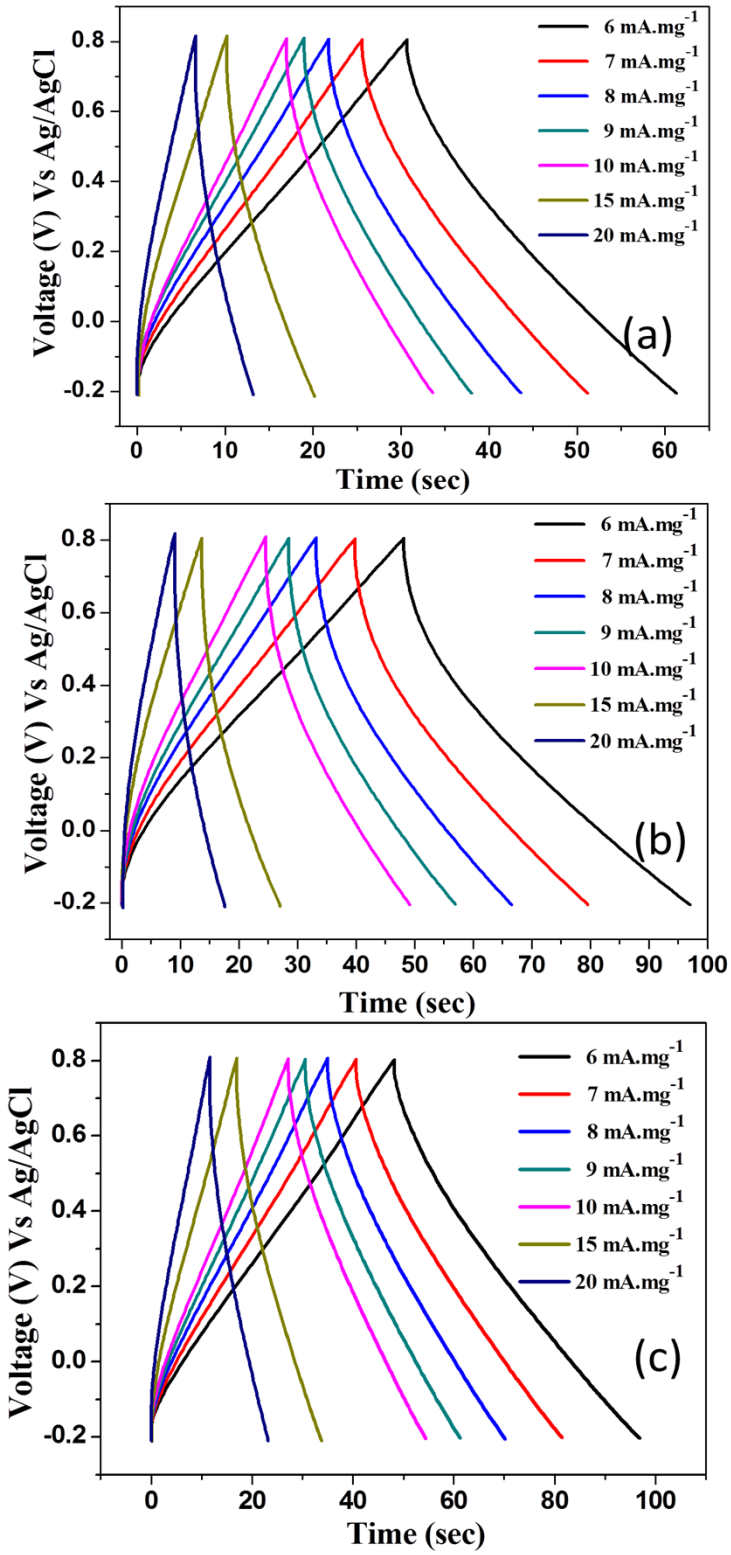

Fig. S6 High rate charge-discharge perfromance in three electrode cell for (a) CNR, (b) HCNR and (c) ACNR sample, respectively.

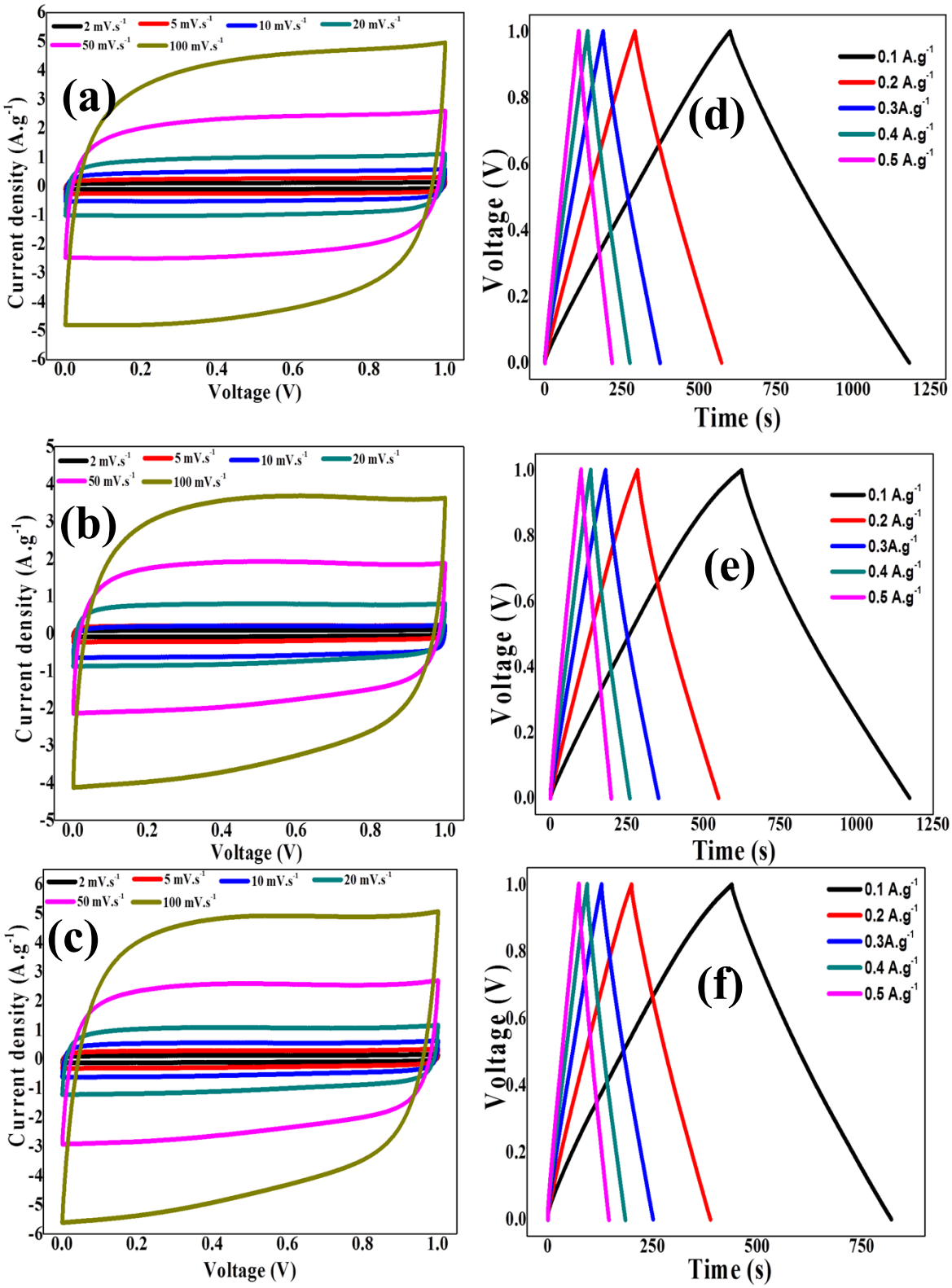

Fig. S7 The symmetric two electrode cell electrochemical anlaysis: (a) – (c) are CVs of ACNR, HCNR and CNR, respectively and (d) – (f) are galvanostatic charge-discharge profiles of ACNR, HCNR and CNR, respectively.

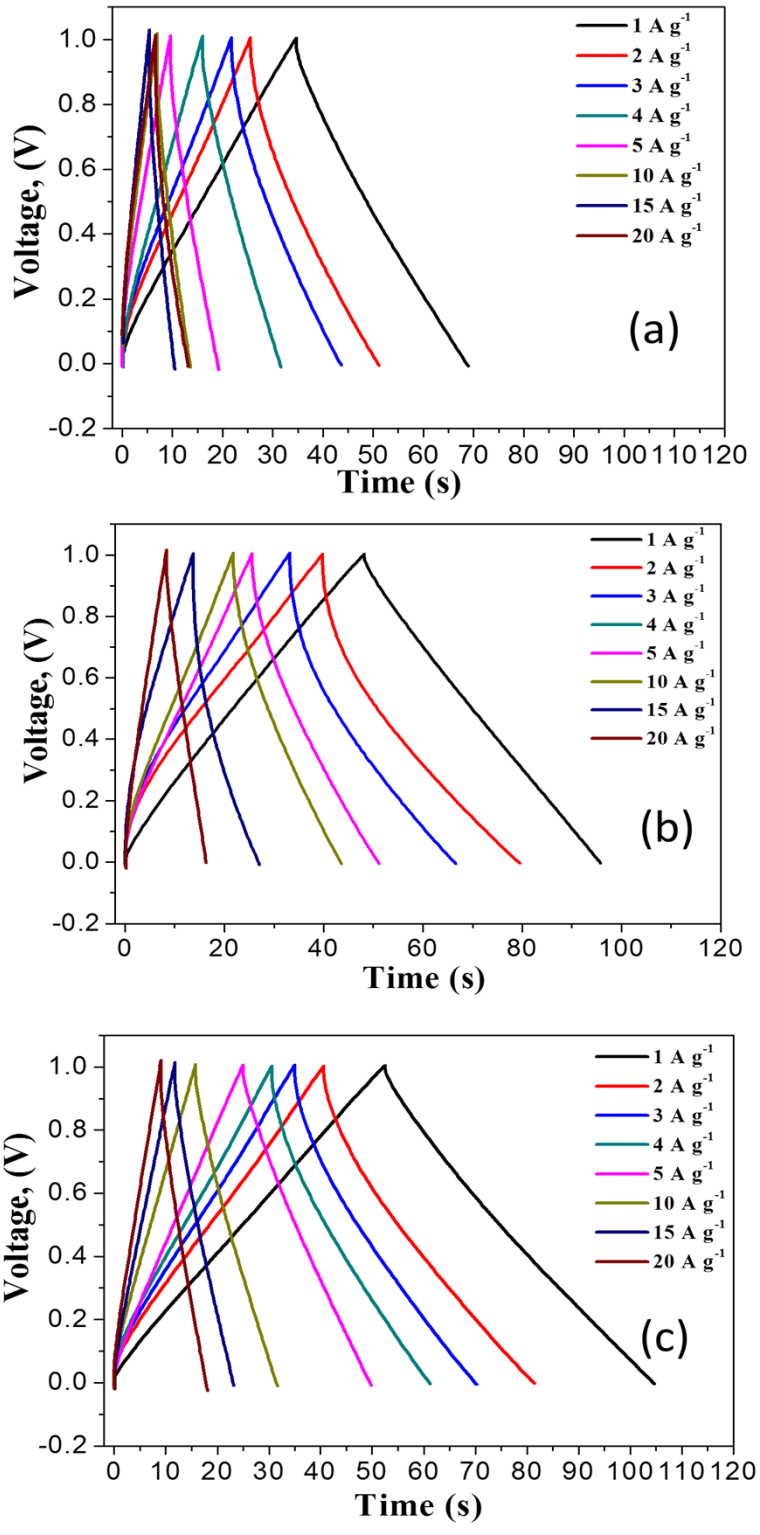

Fig. S8 High rate charge-discharge in two electrode cell for (a) CNR, (b) HCNR and (c) ACNR sample, respectively.

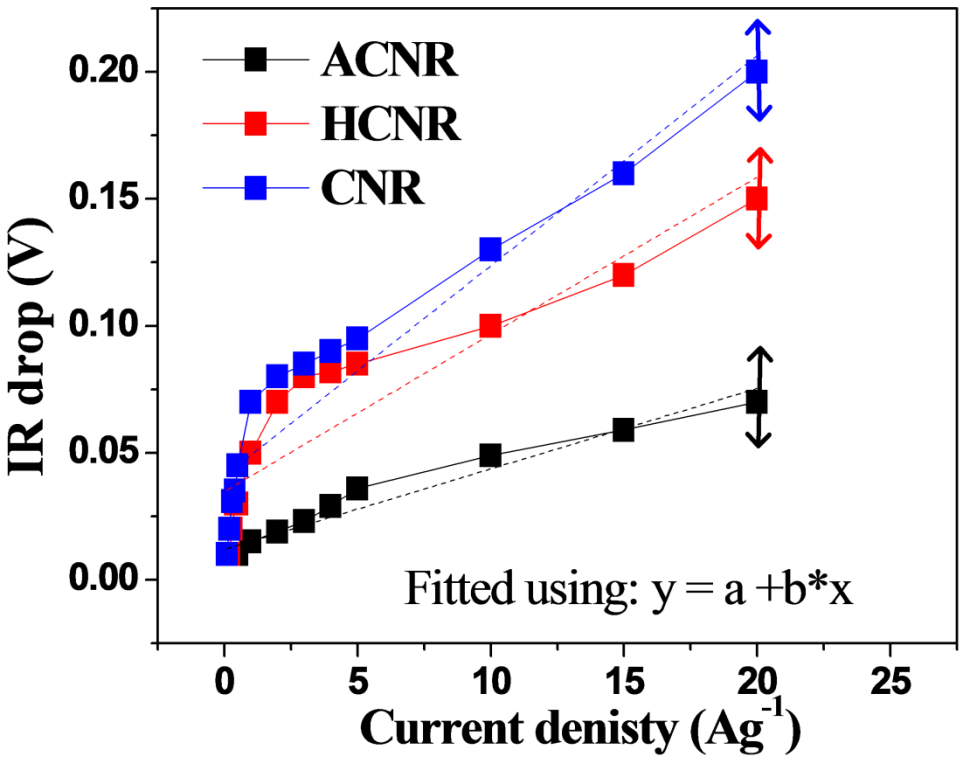

Fig. S9 Variation of IR drop with increase in current densities for all the samples perfromend in two electrode test.

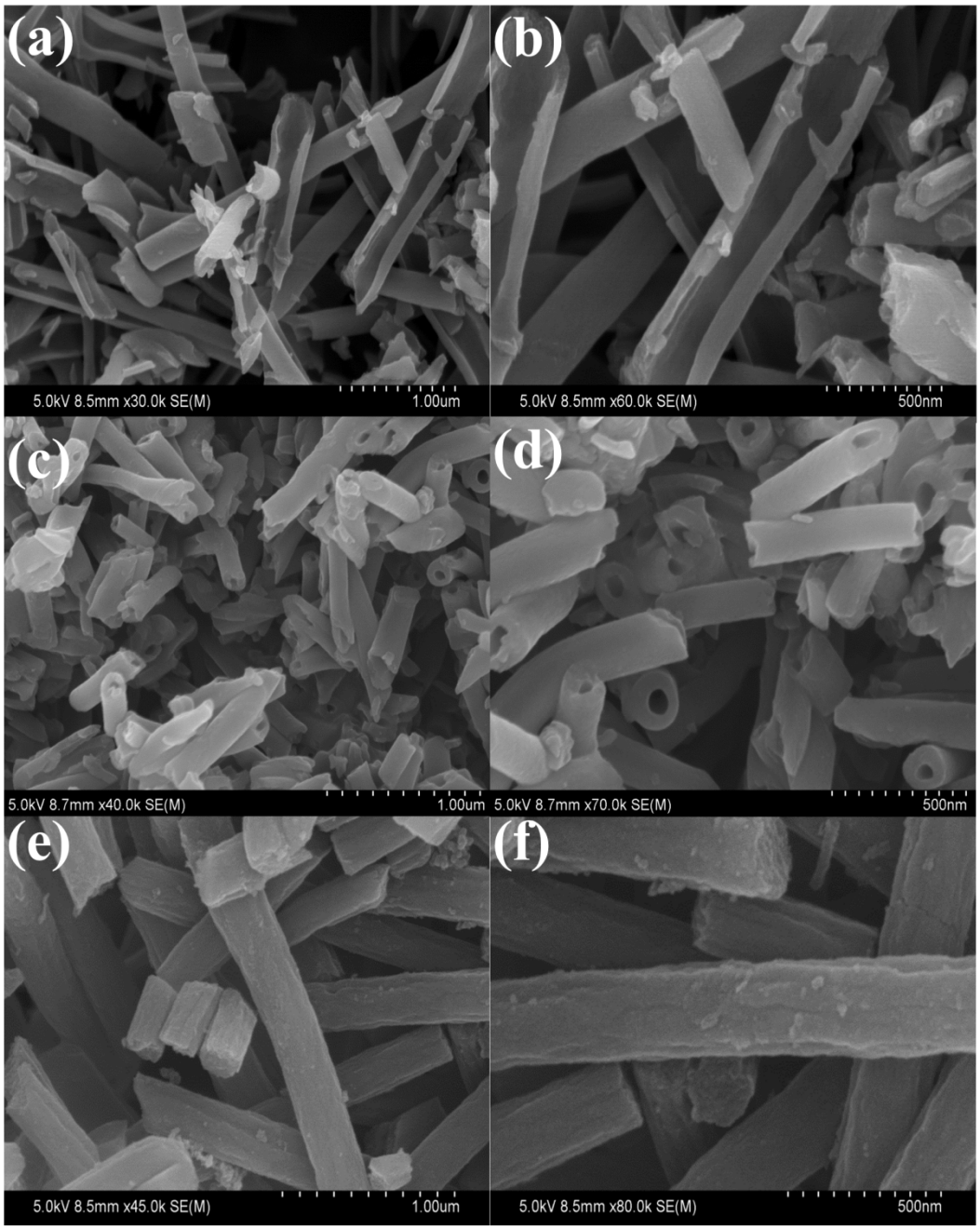

Fig. S10 FE-SEM images of 5000 cycled cell electodes of ACNR (a, b), HCNR (c, d) and CNR (e, f) samples, respectively.

Table S4. Comparisons of previous reports in N-doped carbon materials evaluated in two electrode systems and performed in acidic electrolyte medium.

N –carbon/ N-free carbon materials	$[H_2SO_4]$	C_{sp}, ($F\ g^{-1}$)	Cycle test	E ($Wh\ kg^{-1}$)	Ref.
N- carbon nanocages	0.5	262	5000	8.6	[3]
N-mesoporous carbon	1	262	---	---	[4]
N-mesoporous carbon	2	293	1000	27.4	[5]
N-mesoporous carbon	3	203	---	---	[6]
N-hollow carbon spheres	2	306	1000	---	[7]
N -carbon nanofiber paper	1	200	5000	6	[8]
N-porous carbon	1	300	---	---	[9]
N-activated porous carbon	1	202	---	4	[10]
N-free Porous carbon	1	221	---	6	[2]
N-doped porous HCNR	1	230	5000	7.5	This work
N-doped porous ACNR	1	238	5000	8.4	This work

Supporting information references:

1. M. D. Stoller and R. S. Ruoff, *Energy Environ. Sci.*, 2010, **3**, 1294.

2. L. Estevez, R. Dua, N. Bhandari, A. Ramanujapuram, P. Wang, and E. P. Giannelis, *Energy Environ. Sci.*, 2013, **6**, 1785.

3. Y. Tan, C. Xu, G. Chen, Z. Liu, M. Ma, Q. Xie, N. Zheng, and S. Yao, *ACS Appl. Mater. Interfaces*, 2013, **5**, 2241–8.

4. J. Wei, D. Zhou, Z. Sun, Y. Deng, Y. Xia, and D. Zhao, *Adv. Funct. Mater.*, 2013, **23**, 2322–2328.

5. Z. Lei, X. Sun, H. Wang, Z. Liu, and X. S. Zhao, *ACS Appl. Mater. Interfaces*, 2013, **5**, 7501–8.

6. H. Chen, F. Sun, J. Wang, W. Li, W. Qiao, L. Ling, and D. Long, *J. Phys. Chem. C*, 2013, **117**, 8318–8328.

7. F. Ma, H. Zhao, L. Sun, Q. Li, L. Huo, T. Xia, S. Gao, G. Pang, Z. Shi, and S. Feng, *J. Mater. Chem.*, 2012, **22**, 13464.

8. E. Ra, E. Raymundo-Piñero, Y. Lee, and F. Béguin, *Carbon N. Y.*, 2009, **47**, 2984–2992.

9. M. Seredych, D. Hulicova-Jurcakova, G. Q. Lu, and T. J. Bandosz, *Carbon N. Y.*, 2008, **46**, 1475–1488.

10. E. Frackowiak, G. Lota, J. Machnikowski, C. Vix-Guterl, and F. Béguin, *Electrochim. Acta*, 2006, **51**, 2209–2214.